

Controllable Leidenfrost glider on a shallow water layer

Hideyuki Sugioka, and Satoru Segawa

Citation: *AIP Advances* **8**, 115209 (2018); doi: 10.1063/1.5051238

View online: <https://doi.org/10.1063/1.5051238>

View Table of Contents: <http://aip.scitation.org/toc/adv/8/11>

Published by the *American Institute of Physics*



Don't let your writing
keep you from getting
published!

AIP | Author Services

Learn more today!

Controllable Leidenfrost glider on a shallow water layer

Hideyuki Sugioka^a and Satoru Segawa

Department of Mechanical Systems Engineering, Shinshu University, 4-17-1 Wakasato, Nagano 380-8553, Japan

(Received 7 August 2018; accepted 30 October 2018; published online 9 November 2018)

Levitation and self-propelled functions of the Leidenfrost phenomena are attractive. In this study, we propose a Leidenfrost glider having a ratchet-like topology under its body along with the driving method using the asymmetrical viscous vapor flow, as a prototype of a future vehicle that can move on a flat shallow layer freely. We observed that this vehicle can be accelerated to the velocity of approximately 0.2 m/s on a shallow water layer and the direction can be quickly controlled by changing the center of gravity of the vehicle. Our device might be important to reduce the worldwide energy loss of vehicles or to develop innovative microfluidic transportation systems in the future. © 2018 Author(s). All article content, except where otherwise noted, is licensed under a Creative Commons Attribution (CC BY) license (<http://creativecommons.org/licenses/by/4.0/>). <https://doi.org/10.1063/1.5051238>

Leidenfrost phenomenon is a kind of film boiling and it is characterized by the levitation and long life time of a liquid droplet on a hot plate because of the existence of the Leidenfrost vapor layer between the liquid and the hot plate.^{1,2} In 2006, Linke et al.³ showed that liquids perform self-propelled motion of the level of ~5 cm/s on the hot surface having ratchet-like topology and suggested innovative pumps with no moving part and no external power supply.³ This self-propelled phenomenon accompanying the levitation phenomenon has attracted much attention because of the interest of the fundamental physics^{4,5} and the wide range of new applications,^{6–8} ranging from the macroscopic energy reduction systems⁸ to the microfluidic applications.³ For example, Ok et al.⁴ experimentally showed that the droplet velocity significantly increases as the ratchet period decreases, reaching ~0.4 m/s for submicron ratchet. Li et al.⁵ theoretically showed that the self-propelled motion of Leidenfrost droplet originates from the asymmetry of the ratchet and the vapor flows below the droplets. Further, Hashmi et al. demonstrated that a small cart also can be levitated by Leidenfrost vapor and can move on a hot ratchet surface.^{8,9} In particular, a study on a Leidenfrost transportation system is challenging since it may provide not only a means to reduce a worldwide energy loss due to the friction of the macroscopic vehicle but also a means of a new high-speed transportation system in microfluidic applications, as pointed out by Hashmi et al.⁸ and Linke et al.³ However, to reduce an energy consumption, a heat engine should be equipped on the side of vehicle not on the side of a road (or rail) and the direction of the vehicle should be controllable to move on a flat panel freely for the wide range of applications. Further, to overcome the water supply problem of Hashmi et al.'s cart, we consider a transportation system consisting of a vehicle using a Leidenfrost phenomenon and a shallow water layer. Thus, in this study, we propose a Leidenfrost glider having a ratchet-like topology under its body along with the driving method using the asymmetrical viscous vapor flow owing to the changing of the position of the burden and experimentally prove the performance and functions. In particular, we here demonstrate that the Leidenfrost glider can be accelerated to the velocity of approximately 0.2 m/s on a shallow water layer and the moving direction can be controlled quickly by changing the center of gravity of the vehicle.

Figure 1 shows a experimental setup of the controllable Leidenfrost glider on a shallow water layer. As shown in Fig. 1(a), we placed the heated aluminum vehicle of the mass $m = 1.8$ g at the temperature $T_h = 300$ °C on a flat melamine table that has a shallow water layer of a room temperature

^aElectronic mail: hsugioka@shinshu-u.ac.jp

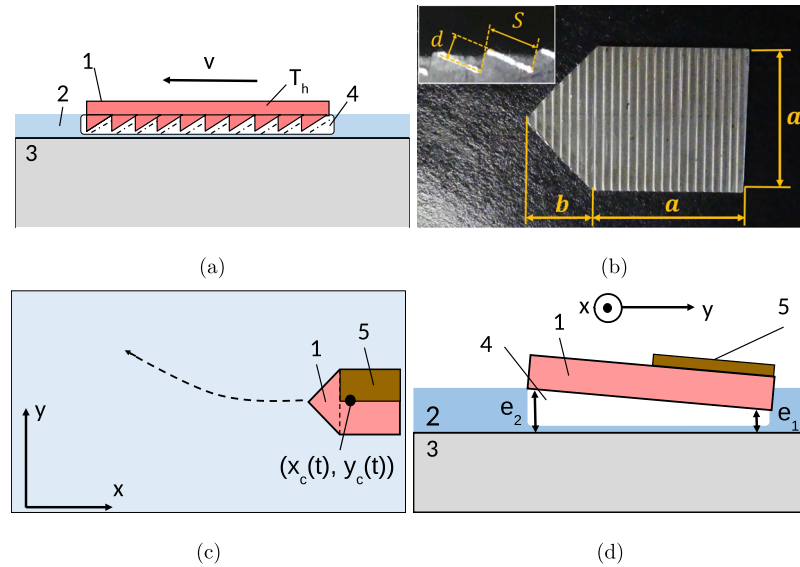


FIG. 1. Experimental setup of the Controllable Leidenfrost glider on a shallow water layer. (a) Propulsion of the Leidenfrost glider. (b) Photograph of the ratchet structure. Here, $a = 2$ cm, $b = 1$ cm, $d = 0.3$ mm, and $S = 1.2$ mm. (c) Control method of the cart direction. The vehicle turns to the right by setting the copper burden on the right half position of the body. (d) Control method of the cart direction. The vehicle turns to the right by setting the copper burden on the right half position of the body. 1: body of the glider having a ratchet structure of the mass of $m = 1.8$ g at the temperature $T_h = 300$ °C, 2: shallow water of the depth $d_w \sim 0.2$ mm, 3: flat table, 4: Leidenfrost vapor layer, and 5: square-shape copper burden of the mass of $m' = 0.7$ g of the thickness of 0.5 mm.

and depth $d_w \sim 0.2$ mm. Then, we observed the motion and determined the center position $(x_c(t), y_c(t))$ at time t by using video data of size 1280×720 with a frame rate of 240 fps. Here, the vehicle of total thickness 1.5 mm has a ratchet under the body and the heat of the ratchet evaporates the water. Consequently, the asymmetrical flow of the Leidenfrost vapor layer is generated and thus, the vehicle is propelled on a shallow water. Note that the asymmetrical vapor flow of this device originates from surrounding water, whereas that of Linke et al.'s device³ originates from water of a droplet above a ratchet. Further, by using a much larger pool (of width 18 cm and length 39 cm) than the vehicle, the water layer thickness was controlled and maintained to $d_w \sim 0.2$ mm, which is comparable to the tooth height of the ratchet ($d_s \approx 0.29$ mm). Here, if the water layer is not thin (i.e., $d_w > d_s$), the drag force of the vehicle becomes large and the heat flux becomes small because of the increasing of the surface area that contacts to water. Thus, the vehicle supposedly becomes difficult to move at $d_w > d_s$. In fact, we could not observe the gliding motion at $d_w \sim 1$ mm (on an acrylic board); it just showed a nuclear boiling phenomenon at the same position. Figure 1(b) shows the photograph of the ratchet of width $w = a = 2$ cm and total length $a + b$, which consists of the front part length $b = 1$ cm and the back part length $a = 2$ cm. Here, the period S of the ratchet is 1.2 mm and the depth d is 0.3 mm, as shown in the inset of Fig. 1(b). Figure 1(c) shows the direction control method of the vehicle, which initial center of gravity is (x_c, y_c) . As shown in Fig. 1(c), we can make the vehicle turned to the right (left) by setting the square-shape copper burden of the mass of $m' = 0.7$ g on the right (left) half position of the body. Namely, by changing the center of gravity of the vehicle, the direction of the motion can be controlled.

Figure 1(d) shows the direction control mechanism. As discussed by Biance et al.,¹ the thickness of Leidenfrost layer e is the function of the total mass $m'' = m + m'$; i.e., $e = f(m'')$. However, as shown in Fig. 1(d), the thickness (e_1) of Leidenfrost layer in R_1 becomes smaller than that (e_2) in the left-side region (R_2) owing to the stacked burden in the right-side region (R_1). Consequently, the drag force $f_1 \sim \mu \frac{v}{e_1} s_c$ due the viscosity of the Leidenfrost layer in R_1 becomes larger than that $f_2 \sim \mu \frac{v}{e_2} s_c$ in R_2 . Thus, the torque $T_L \sim \frac{1}{2}(f_1 - f_2)a$ is generated and it makes the vehicle turned to the burden side. Here, v is the velocity of the vehicle and μ is usually the viscosity of the vapor phase; i.e., $\mu_v = 0.0166$ mPa s at the average temperature $T_L = 200$ °C of the Leidenfrost layer. However,

in a small levitation state at low velocities, the inclination of the body due to the burden results in the partial contact between the water and edge of the burden side. Thus, the drag force of the burden side becomes extremely larger than that of the other side because of the viscosity of the liquid phase; i.e., $\mu_l = 0.285 \text{ mPa s}$ at the boiling point $T_b = 100 \text{ }^\circ\text{C}$ of the thin liquid water layer. Namely, a large torque, which causes a quick turn of a very small radius of curvature, is generated at low velocities. Note that the shift of the center of gravity generates another turning torque $T_u \sim f'_1 l_1 - f'_2 l_2$, where f'_1 and f'_2 are the average Leidenfrost propulsion forces in R_1 and R_2 , respectively; l_1 and l_2 are the average distances between the center of the gravity and the positions of the average forces in R_1 and R_2 , respectively. Although T_u also makes the vehicle turned to the burden side, we consider that it only causes a slow turn of a large radius of curvature as will be discussed later.

Figure 2 shows the photographs of the typical motions of the vehicle. On the one hand, we find that the vehicle without the burden can move approximately straight, as shown in Figs. 2(a) to 2(c). Note that a triangle-shape front was needed to avoid unstable motions and by this device, we could observe symmetrical ripples on a water surface in Fig. 2(b). On the other hand, we observed that the vehicle that stacks the burden on a right (left) position turned right (left) as shown in Figs. 2(d) to 2(f) [Figs. 2(g) to 2(i)]. Note that same experiments were performed three or four times under the same burden condition. Figure 3 shows the characteristics of the controllable Leidenfrost glider. Specifically, Fig. 3(a) shows the dependence of the travel distance $r = \sqrt{x_c^2 + y_c^2}$ on t , and Fig. 3(b) shows the dependence of the velocity $v = \frac{dr}{dt}$ on t . From Figs. 3(a) and 3(b), we find that the vehicle is accelerated until $\sim 0.3 \text{ s}$, and it keeps the constant velocity at approximately $0.3 < t < 0.6 \text{ s}$. Then, it is decelerated and stopped at $t \sim 0.8 \text{ s}$ because of the cool-down of the vehicle. Further, Fig. 3(c) shows the trajectories of the vehicle at the straight, right, and left burden conditions. From Fig. 3(c), we find that the propulsion direction of the Leidenfrost glider can be controlled by shifting the center

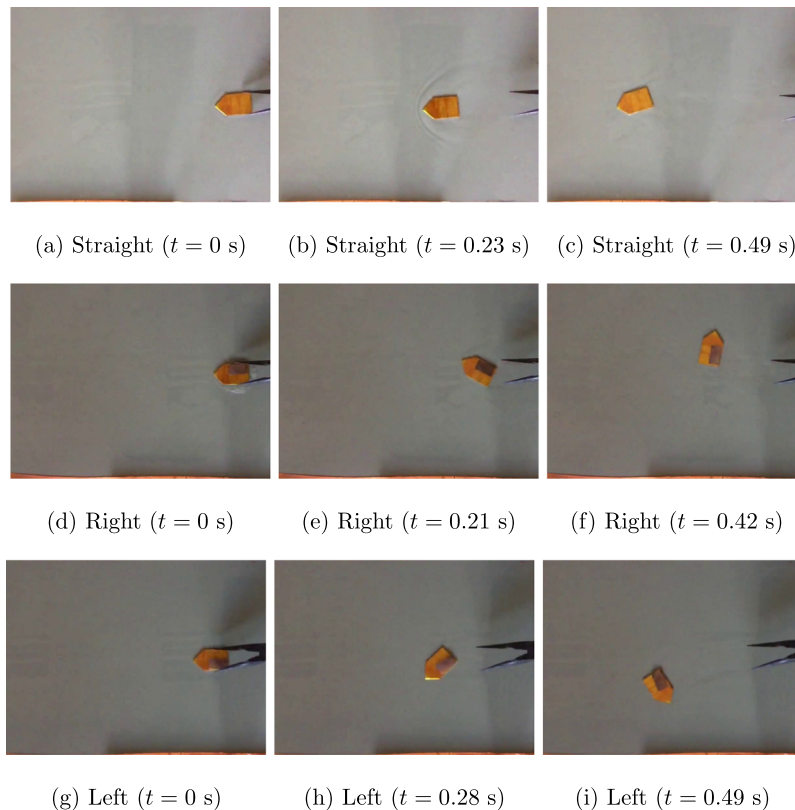


FIG. 2. Photographs of the typical motions of the Leidenfrost glider. (a) to (c): Strait motion of $N = 2$, (d) to (f): Right turn motion of $N = 3$, and (g) to (i): Left turn motion of $N = 3$, where N represents the trial number in the each experiment.

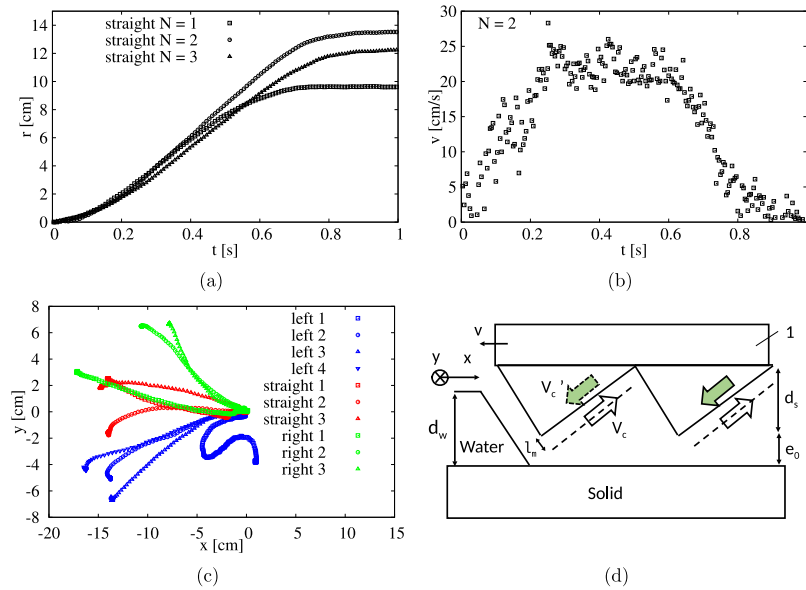


FIG. 3. Characteristics of the controllable Leidenfrost glider. (a) Dependence of r on t for straight motions ($N = 1$ to 3). (b) Dependence of v on t for straight motion ($N = 2$). (c) Trajectory of the vehicle for straight, left-, and right-turn motions ($N = 1$ to 3 or 4). (d) Asymmetrical vapor flow due to thermal creep. Here, $d_w \sim 0.2$ mm, $m = 1.8$ g, $m' = 0.7$ g, $T_h = 300$ °C, $a = 2$ cm, $b = 1$ cm, $d = 0.3$ mm, and $S = 1.2$ mm. In (d), the broken line show the boundary layer of thickness l_m .

of the gravity to some extent, although large experimental variation exists. In particular, we observed an unstable left-turn motion at $N = 1$ in Fig. 3(c). Further, in Fig. 3(c), we find that quick turns appear in an early stage at low velocities, as predicted. Thus, we consider that in the short distance range, the direction of the vehicle is mainly controlled by the torque due to the unbalance of drag forces (T_L) rather than the torque due to the unbalance of propulsion forces (T_u).

Hashmi et al.'s cart is placed on a Leidenfrost droplet that is proven to move by the hot ratchet. However, the motion of our glider was not obvious since intrinsically there exist several different points between Linke et al.'s device and our device. Firstly, we cannot expect large water cushion on the peak position of the ratchet in our device; thus, there was a possibility that the solid ratchet contacts with the surface of the table and the levitation force is not generated. Note that usually the Leidenfrost pressure difference is estimated as $\Delta P_1 \approx mg/A$ (~ 35 Pa)³ and thus the expelling force for water is $F_1 \approx \Delta P_1 e l$, where A ($= a^2 + \frac{1}{2}ab = 5$ cm²) is the bottom area of the vehicle, e is the thickness of the Leidenfrost vapor layer, and l ($= 3a + \sqrt{a^2 + 4b^2}$) is the perimeter of the vehicle. Since the bottom static pressure due to the surrounding water is $\Delta P_2 \approx \rho g d_w$ (~ 2 Pa) and the entering force is $F_2 \approx \Delta P_2 e l$, the water is assumed to be expelled. Secondly, the continuous water supply is not obvious since the liquid water should be entered from an outside region under the existence of the reverse vapor flow due to the Leidenfrost phenomenon. Thirdly, it seems that the large drag force in the front part owing to the water of depth ~ 0.2 mm is inevitable; thus, there was a possibility that it reduces the velocity of the vehicle seriously. Nevertheless, we surprisingly observed the large maximum velocity of ~ 0.2 m/s, which is comparable with that of the devices having the Linke et al.'s configuration; e.g., the maximum velocity of Hashmi et al.'s cart⁸ is approximately 0.16 m/s. This means that (i) in our device, the levitation force is generated at the peak position of the ratchet in spite of the shortage of the water in the quasi-contact region; (ii) the continuous supply of water is realized; (iii) the drag force in the front part due to the propulsion in a shallow water does not affect seriously to the maximum velocity of our device.

Moreover, although a liquid droplet above the ratchet moves in the inclined direction of the ratchet tooth,³ our vehicle experimentally moved in the opposite direction [in the $-x$ direction in Figs. 1 and 3(d)]. This is a surprising result since the asymmetrical viscous vapor flow due to the ratchet structure should drive both our vehicle and the droplet in the same direction, if the asymmetrical viscous vapor flow is the only main mechanism. In other words, to explain the experimental direction

of our vehicle, we need to assume the other mechanism in addition to the asymmetrical viscous vapor flow model. For example, the thermal-creep model that was proposed by Würger¹⁰ seems to explain the both motions of the droplet and our vehicle, although the mechanism should be examined more in the future; i.e., the thermal-creep velocity V_c of the order of ~ 0.2 m/s due to the large thermal gradient along to the ratchet slope¹⁰ in Fig. 3(d) seems to explain the experimental results. That is, for our glider in the shallow water, V_c causes the opposite velocity component V'_c because of Newton's 3rd law and thus our vehicle moves in the $-x$ direction in Fig. 3(d). For Linke et al.'s device, V_c drives a liquid droplet in the inclined direction of the ratchet tooth, although the asymmetrical viscous flow also might contribute to the results to some extent.

Furthermore, Leidenfrost theory usually considers the balance between the rate of evaporation due to the thermal conduction and the rate of evaporation due to the Poiseuille flow.¹ However, if we can assume the thickness of the Leidenfrost vapor layer as $e \sim d_w/2 \sim 100 \mu\text{m}$, the rate of evaporation due to the thermal conduction is simply determined as $\frac{dm_v}{dt} \approx \lambda_v \frac{\Delta T}{e} A \frac{1}{L}$ and the energy use of our glider of weight $m = 1.8$ g per meter is simply estimated as $Q_L \sim \lambda_v \frac{\Delta T}{e} A \frac{1}{v} \sim 32.8$ J/m, whereas the energy use of an ordinary car of weight $m_c \sim 0.5$ t is $Q_c \sim 3340$ J/m since the fuel consumption of the car is approximately 10 km/l. Here, L is the latent heat of evaporation, $\Delta T = T_h - T_b = 200$ K, $\lambda_v = 0.0328$ W/(m K) is the thermal conductivity of the vapor layer at 200 °C, the energy of one liter of gasoline is ~ 33.4 MJ, and $v \approx 0.2$ m/s. Thus, the energy use per meter and kilogram of our glider [$Q_L/m \sim 18.2$ kJ/(m kg)] is much larger than that of the ordinary car [$Q_c/m_c \sim 6.68$ J/(m kg)] in spite of $Q_L \ll Q_c$. Therefore, there is a long way to reduce the worldwide energy loss in spite of its potentiality, and we need to improve ability to lift heavy objects in the future, although the current technology is still useful for microfluidic applications.

In conclusion, we have proposed a Leidenfrost glider having a ratchet-like topology under its body. Further, we have surprisingly demonstrated that the vehicle can move at the velocity of approximately 0.2 m/s on a shallow water layer and the direction of the motion can be controlled by changing the center of gravity of the vehicle.

This work was partially supported by JSPS KAKENHI Grant Number JP16K05650.

¹ A.-L. Bianco, C. Clanet, and D. Qur, *Physics of Fluids* **15**, 1632 (2003).

² D. Quéré, *Annual Review of Fluid Mechanics* **45**, 197 (2013).

³ H. Linke, B. J. Alemán, L. D. Melling, M. J. Taormina, M. J. Francis, C. C. Dow-Hygelund, V. Narayanan, R. P. Taylor, and A. Stout, *Phys. Rev. Lett.* **96**, 154502 (2006).

⁴ J. T. Ok, E. Lopez-Oña, D. E. Nikitopoulos, H. Wong, and S. Park, *Microfluidics and Nanofluidics* **10**, 1045 (2011).

⁵ Q. Li, Q. J. Kang, M. M. Francois, and A. J. Hu, *Soft Matter* **12**, 302 (2016).

⁶ T. R. Cousins, R. E. Goldstein, J. W. Jaworski, and A. I. Pesci, *Journal of Fluid Mechanics* **696**, 215227 (2012).

⁷ G. G. Wells, R. Ledesma-Aguilar, G. McHale, and K. Sefiane, *Nature Communications* **6**, 639 (2015).

⁸ A. Hashmi, Y. Xu, B. Coder, P. A. Osborne, J. Spafford, G. E. Michael, G. Yu, and J. Xu, *Scientific Reports* **2**, 797 (2012).

⁹ A. Hashmi, B. C. G. Yu, Y. Xu, J. Spafford, G. E. Michael, and P. A. Osborne, *Fluids and Heat Transfer, Parts A, B, C, and D* **7**, 2713 (2012).

¹⁰ A. Würger, *Phys. Rev. Lett.* **107**, 164502 (2011).